Evaluating the properties of nucleating liquid drops by Monte Carlo simulation

Author: Adrián Llamas Jaramillo, allamaja@ub.edu
Facultat de Física, Universitat de Barcelona, Diagonal 645, 08028 Barcelona, Spain.

Advisors: David Reguera López, dreguera@ub.edu — Ivan Latella, ilatella@ub.edu

Abstract: Nucleation is the mechanism controlling first order phase transitions and involves the formation of a small critical cluster. Its energy of formation dictates the nucleation rate, but it is difficult to evaluate since the critical cluster is unstable. Here, we develop a new Monte Carlo simulation technique to study the properties of critical droplets and compute their free energy of formation. In particular, we studied a Lennard-Jones fluid with truncated and shifted potential at 2.5 σ (LJTS(2.5 σ)), confined in a small volume at reduced temperature $T = 0.625$. We compare our results for the work of formation to previous data for this system obtained with Umbrella Sampling (US), obtaining good agreement. Our findings suggest that this new technique is particularly promising for investigating small critical clusters relevant to experimental conditions and complex atmospheric fluids, where traditional methods are computationally demanding.

Keywords: Phase transitions, Nucleation, Condensation, Lennard-Jones fluids, Monte Carlo simulations.
SDGs: 6 and 13 (see page 6).

I. INTRODUCTION

One of the main challenges in modern physics is the study and characterization of nano-systems. These systems are very important in different areas such as molecular biology or nanotechnology and are distinguished for having typically a small number of molecules, far from the usual thermodynamic limit. However, they can be properly described by the thermodynamics of small systems [1]. This theory shows how the average properties of a small (even completely open [2]) system can be obtained from an ensemble of *replicas* of the small system. Unlike in macroscopic thermodynamics, the properties of a small system depend on the ensemble defined by the constraints imposed on it.

An important example of those subtleties appears in the context of nucleation. Nucleation is the fundamental mechanism driving first-order phase transitions and is crucial in many scientific and technological contexts. It involves the formation of an unstable critical cluster or nucleus, whose size and energy dictate the onset and rate of phase transformation. A primary challenge in nucleation theory is to accurately determine the work of formation of this critical embryo, as the nucleation rate depends exponentially on this quantity. Even minor inaccuracies in its value can lead to deviations of several orders of magnitude between theoretical predictions and experimental results. However, since the critical cluster is unstable, it is difficult to evaluate its properties by experiments or simulations.

In this work, we introduce a novel simulation technique to evaluate the free energy of formation and properties of small critical clusters. Our method is an adaptation of Monte Carlo simulations in a small system with carefully chosen constraints to make the cluster stable, allowing direct simulation of the critical cluster without the need to sample intermediate states or reconstruct the full free energy landscape.

II. THEORETICAL BACKGROUND

A. Drop formation in a small confined system

As a theoretical basis, we want to describe the thermodynamics of formation of a small drop in a confined volume. We will use the *modified liquid drop* (MLD) model introduced in [3], which is built on *classical nucleation theory* (CNT).

Consider a spherical, impermeable and hard boundary of volume V, with N particles at temperature T. The center of mass of the system is fixed at center of the sphere, which sets the origin of coordinates. In order to find the coexistence conditions, suppose that a drop of n particles has formed at the center of mass. The MLD model makes the following simplifying approximations: The drop is spherical, incompressible, with a sharp interface, and the same density and constant surface tension as the bulk liquid, γ; the vapor is treated as ideal.

The internal energies of each phase are given by the fundamental thermodynamic equations:

$$dU_1 = TdS_1 - p_1 dV_1 + \mu_1 dN_1 \tag{1}$$
$$dU_2 = TdS_2 - p_1 dV_2 + \gamma dA + \mu_2 dN_2. \tag{2}$$

where S_i, p_i, V_i, μ_i and N_i are the entropy, pressure, volume, chemical potential and number of particles for the vapor ($i = 1$) and liquid ($i = 2$) phases. The Helmholtz free energy $F = U - TS$ is the proper thermodynamical potential for a system with fixed N, V, T. An infinitesimal change in the free energy can then be expressed as:

$$dF = -\left(p_2 - p_1 - \frac{2\gamma}{r}\right)dV_2 + (\mu_2 - \mu_1)dN_2, \tag{3}$$

since the volume and total number of particles are fixed. At equilibrium $dF = 0$ and we recover the standard mechanical and chemical equilibrium conditions:

$$p_2 - p_1 = \frac{2\gamma}{r}, \tag{4}$$
$$\mu_1 = \mu_2. \tag{5}$$

The chemical potential can be obtained from the Gibbs-Duhem relation for each phase:

$$N_1 d\mu_1 = -S_1 dT + V_1 dp_1, \tag{6}$$
$$N_2 d\mu_2 = -S_2 dT + V_2 dp_2 + A d\gamma. \tag{7}$$

Since we are treating the vapor phase as an ideal gas, integrating Eq. 6 at constant temperature gives:

$$\mu_1(p_1) - \mu_1^{eq}(p_1^{eq}) = k_B T \ln \frac{p_1}{p_1^{eq}}, \tag{8}$$

where $p_1^{eq} = p_2^{eq}$ and $\mu_1^{eq} = \mu_2^{eq}$ are the pressure and chemical potential at coexistence. Integration of Eq. 7 assuming incompressibility and constant γ, yields:

$$\mu_1(p_2) - \mu_1^{eq}(p_1^{eq}) = v_l (p_2 - p_1^{eq}), \tag{9}$$

where $v_l \equiv V_2/N_2$ is the volume per particle in the liquid drop. Subtracting Eq. 9 and Eq. 8 and using the mechanical equilibrium condition (Eq. 4), yields the coexistence condition:

$$k_B T \ln \frac{p_1}{p_1^{eq}} = \frac{2\gamma}{r} v_l + v_l (p_1 - p_1^{eq}). \tag{10}$$

Substituting the implicit dependencies of $p_1(n)$ and $r(n)$ produces a (transcendent) equation for n, which can be solved numerically, with the system's volume V as the control parameter. This equation has two solutions, one corresponding to the stable coexisting drop and the other to the unstable one. Note that, for an N, P, T or μ, V, T system, the equilibrium conditions, Eq. 4 and 5, only have one solution, corresponding to an unstable solution, which is the critical cluster in the context of nucleation.

The free energy of formation of the drop in terms of its size, $\Delta F(n) \equiv F(n) - F(0)$, which is the relevant quantity for nucleation theory, is then (note that $n = N_2$):

$$\begin{aligned} \Delta F(n) = &-n k_B T \ln \frac{p_1}{p_1^{eq}} + \gamma A \\ &+ n(k_B T - v_l p_1^{eq}) + N k_B T \ln \frac{p_1}{p_0}, \end{aligned} \tag{11}$$

obtained by integrating Eq. 3 at constant temperature, assuming that $V_2 = v_l n$ since the drop is incompressible, and defining $p_0 \equiv N k_B T$ as the pressure of the homogeneous supersaturated phase.

Fig. 1a shows the numerical solution of Eq. 10, obtained using the bisection method, for $N = 80$ and $T = 0.625$ for a LJTS(2.5 σ) fluid in *reduced units* (see Appendix A). For large volumes, the system is dilute and the MLD model predicts that there are no coexistence solutions, indicating a homogeneous vapor phase. For volumes smaller than $V_{\text{ev}} \approx 4560\ \sigma^3$, there are two solutions corresponding to a large (stable) and small (unstable) drop. For $V_{\text{co}} \lesssim 389\ \sigma^3$ all the particles are in the liquid phase. Also, Fig. 1b depicts the free energy of formation of the cluster, $\Delta F(n)$, for three different volumes. For small enough volumes, ΔF has two extrema, corresponding to the critical (maximum) and stable (minimum) cluster, respectively. As the volume of the system increases the stable solution also rises, until both extrema disappear at V_{ev} and the drop evaporates.

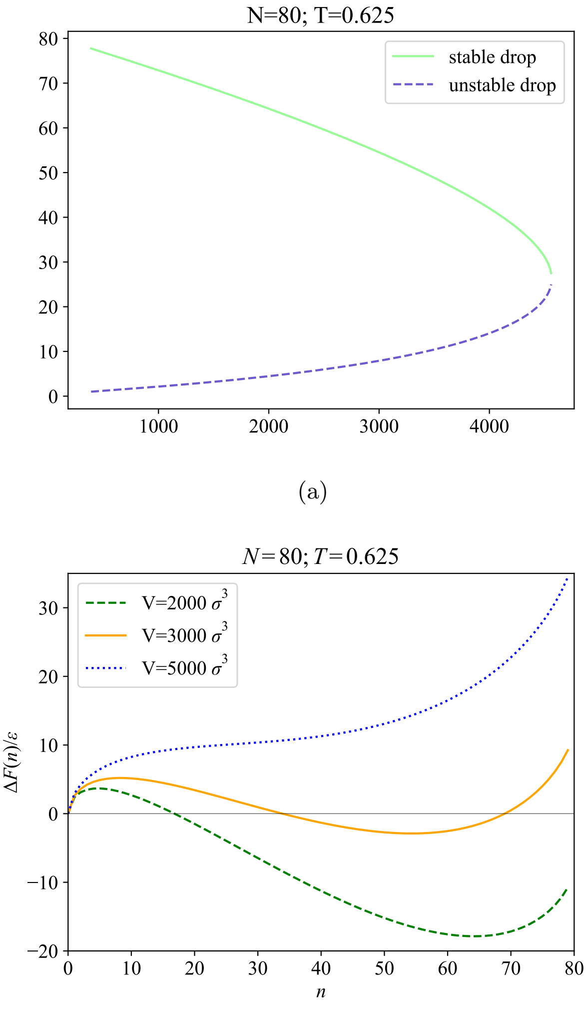

(a)

(b)

FIG. 1: (a) Size of the stable and critical cluster vs volume and (b) free energy of formation vs size for $N = 80$ and $T = 0.625$.

The MLD model predicts the existence of a stable drop in a confined system and the requirements for its stability.

We will now develop a Monte Carlo simulation algorithm to evaluate the properties of this stable drop.

III. MAIN RESULTS

We implemented a Fortran code based on [4] to perform Monte Carlo (MC) simulations in the canonical ensemble for a system of particles interacting with a Lennard-Jones potential truncated and shifted at a reduced cut-off radius of $r_c = 2.5$. MC simulations with $N = 80$ particles were performed at a reduced temperature $T = 0.625$ for different volumes. The simulation box was spherical without periodic boundary conditions and with a fixed center of mass. We stabilized the drop and characterized its average pressure (Fig. 2a), chemical potential (Fig. 2b) and drop size (Fig. 2c) as a function of the system's volume. The number of particles in the drop has been evaluated using a cluster criteria based on distance and number of neighbors. For specific details about how the simulations were done, we refer the reader to Appendix B.

A. Average drop properties

As it can be seen in Figs. 2a-2c, the data presents three distinguishable regions: At high volumes, the system is a dilute homogeneous vapor, the pressure converges towards the equation of state (EoS), the drop size is zero, and the chemical potential monotonically decreases. For $V < 4000\ \sigma^3$, a liquid drop coexisting with its vapor was observed. Figs. 2a and 2c show that, as the volume gets smaller, the size of the drop increases at the expense of its surrounding vapor and the average pressure decreases accordingly, implying a *negative* isothermal compressibility. Such seemingly strange behavior is characteristic of a phase transition in a small confined system, and does not violate any thermodynamic stability condition, as discussed in [3]. For $V \lesssim 500\ \sigma^3$, the system is undergoing a high compression. This is reflected in the exponential increase in the pressure.

B. Radial density profiles

The *radial density profile*, $\rho(r)$, i.e. the average number of particles per unit volume at distance r from the origin, was obtained for every simulation, as a way to characterize the density inside the liquid drop, its interface with the vapor, and to compute the chemical potential (see Appendix B). Fig. 3 shows three distinct representative cases. For $V = 250\ \sigma^3$, the density at the center of the drop lightly exceeds its bulk liquid density and the interface is quite sharp. For $V = 2675\ \sigma^3$, we have a liquid drop with a diffuse interface coexisting with its vapor. Finally, for $V = 4900\ \sigma^3$, the homogeneous distribution denotes a single vapor phase.

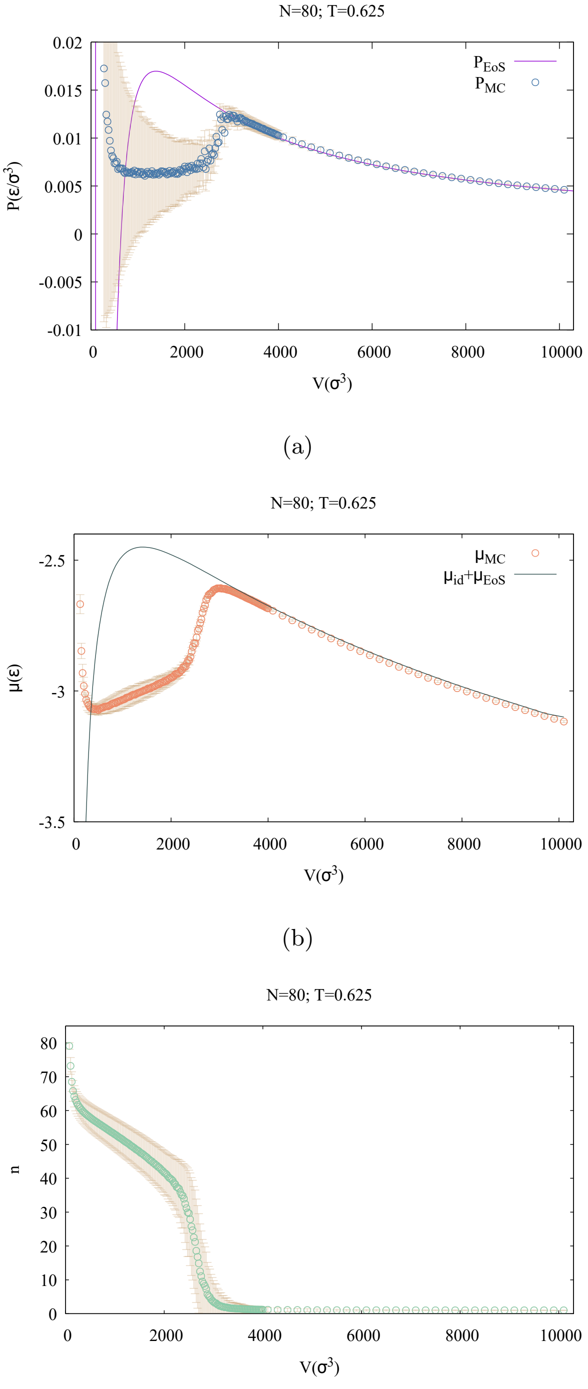

(a)

(b)

(c)

FIG. 2: Average values of the (a) pressure, (b) chemical potential, and (c) number of particles in the drop, as a function of the volume, for $N = 80$ and $T = 0.625$. The dots are the results of the simulations, and the lines represents the values of the EoS for the homogeneous fluid.

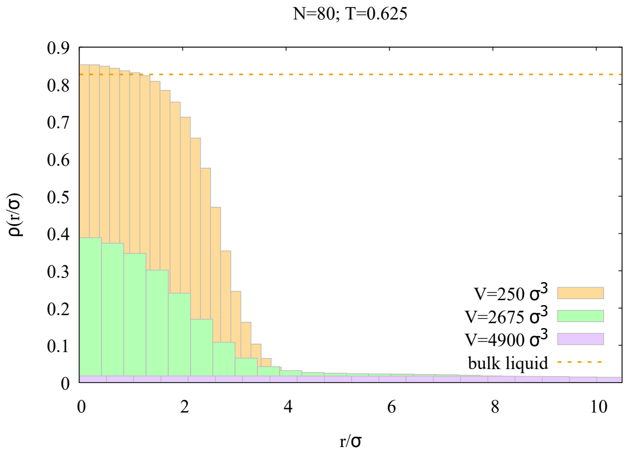

FIG. 3: Radial density profiles for volumes 250 σ^3, 2675 σ^3 and 4900 σ^3 (in purple, at the bottom) for $N = 80$ and $T = 0.625$. All the histogram data-points have uncertainties $\Delta_{\rm STD} \lesssim 10^{-3}$. The bulk liquid density of the LJTS(2.5 σ) is shown as a reference.

C. Free energies of formation

The Helmholtz free energy of formation of the drop was obtained by numerical integration of the Gibbs-Duhem relation:

$$\Delta F(V) = -\int_{V_{\rm max}}^{V} \Big[p_{\rm MC}(V) - p_{\rm EoS}(V)\Big] dV, \tag{12}$$

where the subscripts distinguish between the pressure measured in the MC simulations and data from the EoS for the homogeneous vapor [5], and $V_{\rm max} = 10100\ \sigma^3$ is the largest volume simulated for the homogeneous vapor phase. Eq. (12) represents the free energy of formation of a *stable* cluster coexisting with its vapor at a pressure $p_{\rm MC}$. This cluster fulfills the equilibrium conditions given by Eqs. 4 and 5. If instead of fixing the volume, we fixed the value of the pressure to $p_{\rm MC}$, this cluster , which is stable in the canonical ensemble, will correspond to the critical cluster in the N, P, T ensemble, which is the only solution of Eqs. 4 and 5. Thus, it is possible to calculate the Gibbs free energy of formation of the critical cluster in a supersaturated vapor at $p_{\rm MC}$ from the Helmholtz free energy of the stable cluster, using the thermodynamic relation [6]:

$$\Delta G(V) = \Delta F(V) + V\Delta p(V) - N\Delta\mu(V), \tag{13}$$

where $\Delta p \equiv p_{\rm MC} - p_{\rm EoS}$ and $\Delta\mu \equiv \mu_{\rm MC} - \mu_{\rm EoS}$. Figs. 4 and 6 (see Appendix C) show the Helmholtz and Gibbs free energies of formation as a function of the volume and drop size, respectively.

In Fig. 4, a $\Delta F < 0$ region appears in the $\sim 300 - 3000\ \sigma^3$ range, indicating a stable drop, with a minimum value of $\Delta F_{\rm min} = -15.601\ \varepsilon$ at $V = 725\ \sigma^3$. Conversely, in the same region $\Delta G > 0$. This is in line with the idea that every stable cluster in a system defined by the canonical variables N, V and T, corresponds to an unstable critical cluster in a system N, P, T ensemble.

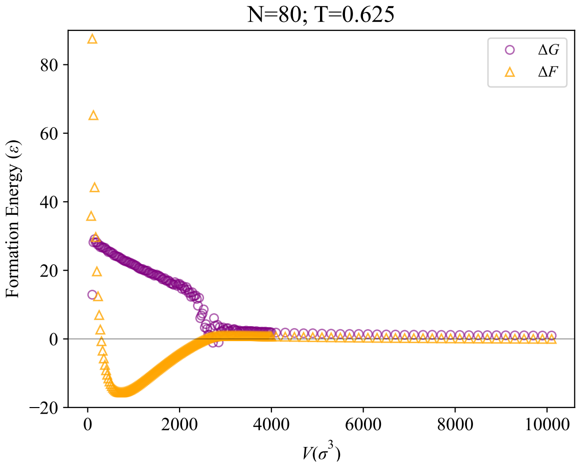

FIG. 4: Drop free energies of formation versus volume, for $N = 80$ and $T = 0.625$.

D. Comparison with Umbrella Sampling

Finally, we contrasted our results with previous data from Umbrella Sampling (US) Monte Carlo simulations in the N, P, T ensemble for the same LJTS(2.5 σ) fluid, evaluating the Gibbs free energy of formation of the critical cluster for different values of the pressure [7], at reduced temperature of $T = 0.625$. In order to make a comparison, the values of the vapor pressure reported in those simulations were converted to the corresponding chemical potential using the EoS for the homogeneous vapor [5].

Fig. 5 shows the comparison between the two datasets. The figure reveals that the Gibbs free energies of formation are in good agreement, particularly in the region of interest $-3 \lesssim \mu/\varepsilon \lesssim -2.8$, where the liquid drop is formed. Nonetheless, for values $\mu/\varepsilon \gtrsim -2.8$, the data seems to change its slope, relative to the US results.

This discrepancy may be due to three main factors. First, in our MC simulations we fixed the center of mass, unlike in the US simulations. Fixing the center of mass removes the translational degrees of freedom of the cluster, which have a contribution to the energy of formation, as discussed in [8]. Second, the use of an EoS as a reference which might be not so accurate for our LJTS(2.5 σ) with a fixed center of mass. Third, a boundary effect caused by working with non-periodic boundary conditions may also be a contributing factor.

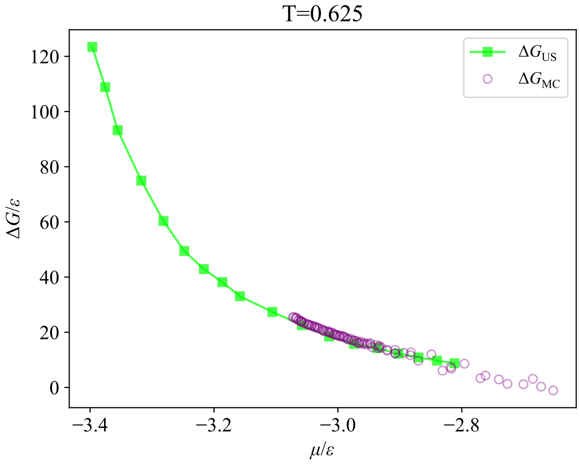

FIG. 5: Comparison between the Gibbs free energy of formation for the US data and our simulations, versus the chemical potential, for a LJTS(2.5 σ) fluid at $T = 0.625$.

IV. CONCLUSIONS

We have studied the formation of a small liquid drop in a confined system. Using the MLD model, we have shown that it is possible to stabilize a drop within the canonical ensemble, to then study its properties and energy of formation. In order to demonstrate this idea, we have performed Monte Carlo simulations for a system of $N = 80$ particles interacting with a Lennard-Jones potential truncated and shifted at 2.5 σ, inside a spherical volume at reduced temperature of $T = 0.625$. We measured the average properties of the cluster, in particular, the pressure, size, density profile, and chemical potential. (We also observed a negative isothermal compressibility, a phenomenon not unique to our small system [3].) From these data, we computed the Helmholtz and Gibbs free energies of formation, showing the correspondence between a stable cluster in the canonical ensemble and a critical cluster in the isobaric-isothermal ensemble. Finally, we contrasted our findings with literature data from Umbrella Sampling simulations, obtaining good agreement.

The interest of the study resides in the context of nucleation, where experiments are typically performed under fixed pressure. In such conditions, the critical cluster, which is the embryo of the new phase, is unstable and estimating its energy of formation ΔG directly would not be possible unless some sort of additional constraint is imposed, as in US simulations. However, these simulations are computationally costly and require a large number of particles. Instead, we have shown that one can stabilize a drop in the canonical ensemble, measure its properties, and then reconstruct the formation energy in the N, P, T ensemble through Eq. 13.

This new simulation method requires few particles, is computationally efficient and will be specially useful in the study of nucleation in fluids with complicated intermolecular potentials.

Acknowledgments

I am deeply grateful to my advisors, Prof. Reguera, for his help, patience and dedication. I am equally grateful to Prof. Latella for his implication and support in this project; I am truly honored to have had the opportunity to work with both of them. I also want to acknowledge Daniel Garrapucho, for his technical assistance with the Superfe Cluster. Finally, I am grateful to my family, girlfriend and friends, for their nurturing during this period.

---

[1] T. L. Hill, *Thermodynamics of Small Systems*, Dover, New York (2013).
[2] I. Latella, A. Campa, L. Casetti, P. D. Cintio, J. M. Rubi, and S. Ruffo, Phys. Rev. E **103**, L061303 (2021).
[3] D. Reguera, R. K. Bowles, Y. Djikaev, and H. Reiss, J. Chem. Phys. **118**, 340-353 (2003).
[4] D. Frenkel and B. Smit, *Understanding Molecular Simulation: From Algorithms to Applications*, Academic, San Diego (2002).
[5] M. Heier, S. Stephan, J. Liu, W. G. Chapman, H. Hasse, and K. Langenbach, Mol. Phys. **116**, 2083-2094 (2018).
[6] D. Reguera and H. Reiss, J. Phys. Chem. B **108**, 19831-19842 (2004).
[7] A. Aasen, Ø. Wilhelmsen, M. Hammer, and D. Reguera, J. Chem. Phys. **158**, 114108 (2023).
[8] K. J. Oh and X. C. Zeng, J. Chem. Phys. **108**, 4683–4684 (1998).
[9] S. Stephan, J. Liu, K. Langenbach, W. G. Chapman, and H. Hasse, J. Phys. Chem. C **122**, 24705 (2018).
[10] N. Metropolis, A. W. Rosenbluth, M. N. Rosenbluth, A. H. Teller, and E. Teller, J. Chem. Phys. **21**, 1087 (1953).
[11] M. P. Allen and D. J. Tildesley, *Computer Simulation of Liquids*, 2nd ed., Oxford (2017).
[12] B. Widom, J. Stat. Phys. **19**, 563–574 (1978).
[13] P. R. ten Wolde and D. Frenkel, J. Chem. Phys. **109**, 9901–9918 (1998).

Avaluació de les propietats de gotes líquides en nucleació per simulació Monte Carlo

Author: Adrián Llamas Jaramillo, allamaja@ub.edu
Facultat de Física, Universitat de Barcelona, Diagonal 645, 08028 Barcelona, Spain.

Advisors: David Reguera López, dreguera@ub.edu — Ivan Latella, ilatella@ub.edu

Resum: La nucleació és el mecanisme que controla les transicions de fase de primer ordre, involucrant la formació d'un petit clúster crític. La seva energia de formació dicta el ritme de nucleació, però és difícil de calcular donat que el clúster crític és inestable. Es desenvolupa una nova tècnica de simulació Monte Carlo per estudiar les propietats mitjanes de gotes petites crítiques i es calcula la seva energia lliure de formació. En particular, es va estudiar un fluid generalitzat de Lennard-Jones amb un potencial truncat i desplaçat a 2.5 σ (LJTS(2.5 σ)), de $N = 80$ partícules confinades en un volum a una temperatura reduïda de $T = 0.625$. Després es comparen els resultats amb dades prèvies per aquest tipus de fluid obtingudes amb Umbrella Sampling. Els resultats suggereixen que aquesta nova tècnica es particularment prometedora per la investigació de clústers petits crítics rellevants en condicions experimentals i fluxos atmosfèrics complexos, on els mètodes tradicionals són computacionalment demandants.
Paraules clau: Transicions de fase, Nucleació, Condensació, Fluid de Lennard-Jones, Simulacions Monte Carlo.
ODSs: Aquest TFG està relacionat amb els Objectius de Desenvolupament Sostenible (SDGs) 6 i 13.

Objectius de Desenvolupament Sostenible (ODSs o SDGs)

1. Fi de la es desigualtats		10. Reducció de les desigualtats	
2. Fam zero		11. Ciutats i comunitats sostenibles	
3. Salut i benestar		12. Consum i producció responsables	
4. Educació de qualitat		13. Acció climàtica	X
5. Igualtat de gènere		14. Vida submarina	
6. Aigua neta i sanejament	X	15. Vida terrestre	
7. Energia neta i sostenible		16. Pau, justícia i institucions sòlides	
8. Treball digne i creixement econòmic		17. Aliança pels objectius	
9. Indústria, innovació, infraestructures			

Appendix A: Lennard-Jones truncated and shifted fluid using reduced units

In this subsection we introduce the Lennard-Jones fluid truncated and shifted at $r_c = 2.5$, that we have used in our simulations.

The Lennard-Jones potential is a popular potential for pairwise particle interaction, for its simplicity to describe repulsion at short distances and attraction at moderate distances. For these reasons, it has been extensively studied in literature, and its EoS has been already characterized [9]. The LJ potential between particles i and j is:

$$U_{\mathrm{LJ}}(r_{i,j}) = 4\varepsilon\left[\left(\frac{\sigma}{r_{i,j}}\right)^{12} - \left(\frac{\sigma}{r_{i,j}}\right)^{6}\right], \qquad \text{(A1)}$$

where σ is the distance at which the potential is zero and ε the energy minimum of the potential well. *Truncating* and *shifting* this potential means that pairwise particle interactions separated longer than the cut-off radius are not computed (truncating) and that we subtract the value of the potential at the cut-off radius from its value at any other point (shifting). Then the LJTS potential is expressed as:

$$U_{\mathrm{LJTS}}(r_{i,j}) = \begin{cases} U_{\mathrm{LJ}}(r_{i,j}) - U_{\mathrm{LJ}}(r_c), & \text{if } r \le r_c \\ 0, & \text{if } r > r_c \end{cases}. \qquad \text{(A2)}$$

For convenience we write $U_{\mathrm{LJTS}}(r_{i,j}) \equiv U_{i,j}$. An important property of this potential is that it has no discontinuities [4].

In our simulations, reduced units were used so that the results may describe an entire set of particular systems (e.g., Ar or Xe) each at some physical temperature and density. All dimensionless quantities were obtained relative to the basic units of the LJ particle's mass, m, and distance σ and energy ε from Eq. A1. For instance, the reduced units of pressure and temperature are σ^3/ε and $k_B T/\varepsilon$, respectively.

Appendix B: Details of the Monte Carlo simulations

Having introduced the LJTS(2.5 σ) in Appendix A, we proceed to explain the statistical-mechanical basis of the Monte Carlo (MC) simulations and the details on how we performed the simulations for this fluid. We applied MC simulations with 10^8 equilibration and production steps, respectively, at volumes ranging from 75 σ^3 to 10100 σ^3. All simulations were done in the *Superfe Computing Cluster*.

In the canonical ensemble, for a *separable* Hamiltonian, the ensemble average $\langle O \rangle$ of an observable $\hat{O}$ is [4]:

$$\langle O \rangle = \frac{\int d^N\mathbf{r}\; e^{-\beta U(\mathbf{r}^N)} \hat{O}(\mathbf{r}^N)}{Z}, \qquad \text{(B1)}$$

where $U(\mathbf{r}^N)$ is the system's energy at state $\mathbf{r}^N$; we assume we can integrate analytically over momenta. The the Metropolis algorithm is used to generate configurations with relative probability $e^{-\beta U(\mathbf{r}^N)}$, to sample configuration space minimizing the energy, converging towards equilibrium. We generated new configurations by random displacements of particles from an initial position $\mathbf{r}_0^N$ to a new one, $\mathbf{r}_1^N$, using the original Metropolis detailed balance rule for the acceptance probability [10]:

$$\mathrm{acc}(\mathbf{r}_0^N \to \mathbf{r}_1^N) \equiv \min(1, \exp\left[U(\mathbf{r}_1^N) - U(\mathbf{r}_0^N)\right]). \qquad \text{(B2)}$$

Then, for each simulation, the program initialized the system as an FCC structure for convenience and corrected its center of mass such that it coincided with the desired origin of coordinates. No periodic boundary conditions were applied [11], since we want to simulate a small confined system.

Once the system was initialized, for each MC step a randomly selected particle was displaced a random distance, up to a maximum, chosen such that on average 50% of the trial moves were accepted. Then, another randomly chosen particle was displaced by the *same* amount but in opposite direction, to maintain the center of mass fixed.

Then the algorithm would accept or reject the change of configuration with acceptance probability given by Eq. B2, with an energy change of δU prior and after displacing particles 1 and 2:

$$\delta U = (\epsilon_1' - \epsilon_1) + (\epsilon_2' - \epsilon_2) - (U_{1,2}' - U_{1,2}), \qquad \text{(B3)}$$

where $\epsilon_i \equiv \sum_{j \neq i} U_{i,j}$.

The pressure was calculated by averaging the virial. In order to measure the chemical potential μ, we implemented the Widom insertion method [12] for a spatially inhomogeneous system, where the chemical potential is calculated as:

$$\mu = k_B T \ln\left(\frac{\rho(\mathbf{r})}{\langle e^{-\beta \delta U(\mathbf{r})} \rangle}\right), \qquad \text{(B4)}$$

We verified that at equilibrium the chemical potential was homogeneous [4]. $\rho(\mathbf{r})$ is the radial density profile. In order to compute it, for a given volume, the system's radius was divided into 20 regular intervals. Then, every 100th MC step, the program sampled each particle's position, sorted it into a bin, and updated its histogram frequency by 1 unit. The procedure would be repeated for all particles. Finally, the histogram was normalized by the shell volume enclosed in each bin.

To measure the drop size (its number of particles), an already existing `C` program was integrated in `Fortran`, which implements the ten Wolde-Frenkel cluster criterion [13]: The program classifies a particle as forming part of a liquid-like cluster if it has 5 or more neighbors within a distance smaller than a cut-off radius (named also Stillinger radius) of 1.5 σ. Both of these parameters have been found to be optimal for this type of simulations [7]. Then the program outputs the biggest found cluster.

Appendix C: Free energies as a function of the cluster size

In this subsection we include additional data obtained from the simulations, presented in Fig. 6. Concretely, we wanted to characterize the free energy of formation as a function of the cluster size, n, to complement the results from Fig. 4 from section III C. In Fig. 6, ΔF is negative in the $\sim 40 - 60$ particle range, which, by inspection of Fig. 2c, corresponds to the $\sim 2000 - 300\ \sigma^3$ volume range, providing further evidence for the presence of a drop. The drop size at the formation energy minimum is $n_{\text{min}} = 55 \pm 4$. As expected, the corresponding values of ΔG are positive.

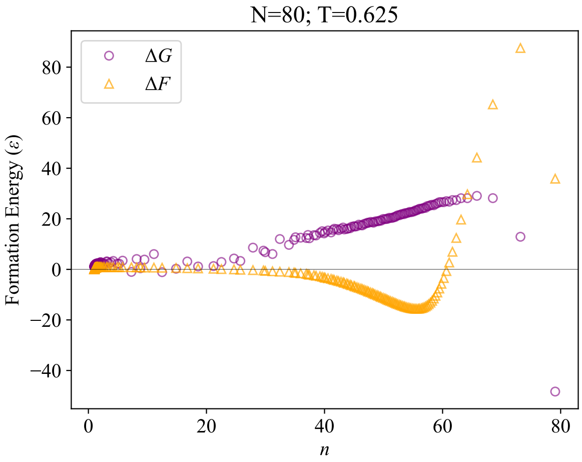

FIG. 6: Drop free energies of formation versus cluster size, for $N = 80$ and $T = 0.625$.